

Redundancy Resolution of Wire-Actuated Parallel Manipulators

Maryam Agahi¹ and Leila Notash²

¹ Department of Mechanical and Materials Engineering, Queen's University, Kingston, ON, agahi@me.queensu.ca

² Department of Mechanical and Materials Engineering, Queen's University, Kingston, ON, notash@me.queensu.ca

Abstract

Kinematically redundant manipulators have potential advantages of using their degree(s) of redundancy to satisfy additional task(s). To achieve desirable performance criteria, various optimization techniques can be applied to redundant manipulators. In the work presented, the redundancy resolution of planar wire-actuated parallel manipulators is investigated at various kinematic and dynamic levels in order to perform desirable tasks while maintaining positive tensions in the wires. Local optimization routines are used in the simulations in order to minimize the norm of actuator forces/torques or to minimize the norm of the mobile platform velocity, subject to positive tension in the wires. This paper presents techniques to alter wire tensions, mobile platform trajectory, mobile platform velocity, and length rate of wires, in order to maintain positive wire tensions. The effectiveness of the presented approaches is studied through simulations of an example planar wire-actuated manipulator. The presented approaches can be utilized in the design of controllers, trajectory planning, and dynamic workspace analysis.

Keywords: Wire-actuated parallel manipulators, redundancy resolution, dynamics, positive wire tension

1. INTRODUCTION

Employing robot manipulators has drawn a considerable attention to repetitive operations, mass production, high precision, and in hazardous environments to assure the accuracy and reduce the cost involved. Redundant manipulators are a considerable research subject in the field of robotics. Kinematically redundant manipulators have more degrees of freedom than are necessary to perform a given task, which means that for a given end effector velocity an infinite number of joint velocities exists. In closed-loop manipulators, redundancy can also be in the form of actuation, if the number of actuated joints is more than the degrees of freedom of the manipulator, then for a given end effector trajectory and external forces/moments, an infinite number of actuator torques/forces exists. Redundant manipulators can use their degree(s) of redundancy to satisfy additional desirable task(s). Redundancy gives the manipulator great versatility and broad applicability to avoid obstacles, avoid structural limitations (e.g., joint limits), minimize joint forces/torques, and avoid singularities (e.g., configurations at which mobility of the manipulator is reduced and it would not be possible to impose an arbitrary motion to the end effector).

A configuration of a manipulator is a complete specification of the location of every point on the manipulator. A manipulator is said to be parallel if its kinematic structure takes the form of a closed-loop chain of links connected by joints. A parallel manipulator consists of a mobile platform (end effector) connected to a fixed base by several branches/legs/limbs. If all links of a manipulator move in a plane or in parallel planes, then the manipulator is called planar. Wire-actuated parallel manipulators are a special kind of parallel manipulator with multiple wires attached to a mobile platform and with the advantage of having larger workspace that the mobile platform can reach, being able to be disassembled and reconfigured, increased manoeuvrability, and being lightweight and transportable. The light weight and the long range of wires allow high speed motion, as well. Wires can only apply force in the form of tension (i.e., pulling the mobile platform but not pushing it). Therefore, to design a fully controllable wire-actuated parallel manipulator, the manipulator has to be redundantly actuated. Thus, at least $n + 1$ wires are required for a manipulator with n degrees of freedom (DOF) to keep positive tension in all wires [1-4].

Various optimization techniques have been applied to resolve redundancy of redundant manipulators. In most redundancy resolution schemes, there are dynamic interactions between the end effector motion and the self-motion (or null-motion) of the manipulator. Self-motion refers to those joint velocities that result in zero motion of the end effector. At the torque level, the null term of actuator forces/torques is interpreted as portions of actuator forces/torques that result in zero forces/moments the end effector could apply/resist. The proper use of the null term is of great importance in redundancy resolution. General kinematic, dynamic and stiffness analyses, as well as, the design of wire-actuated manipulators are investigated in [1-8]. Choe et al. [2] investigated stiffness analysis of a wire-actuated manipulator and proposed a design to reduce vibration caused by the elasticity of wires. Kawamura et al. [1] derived kinematics and dynamics of a high speed wire-actuated parallel manipulator. They analysed the motion stability and investigated the non-linear elasticity of their proposed manipulator. Williams and Gallina [5] introduced translational planar wire-actuated manipulators and presented kinematic, static and dynamic modelling as well as the control architecture. Oh and Agrawal [7] investigated how to design positive tension controllers for wire-actuated manipulators with redundant wires to follow prescribed trajectories. Notash and Kamalzadeh [8] investigated the inverse dynamics of wire-actuated parallel manipulators with a constraining linkage and redundancy in actuation. The workspace of planar wire-actuated parallel manipulators is investigated in [3, 4, 9, 10].

When redundancy in actuation is used, obtaining a unique solution among the infinite inverse dynamic solutions is complicated and needs several considerations such as avoiding negative tensions in wires, reducing the actuator forces/torques, and reducing wire length rates. Therefore, wire actuation and redundancy add more complexity to the inverse dynamics and redundancy resolution in the wire-actuated parallel manipulators. In the presented work, it is attempted to resolve some of the challenges associated with the redundancy resolution of wire-actuated parallel manipulators, benefit from potential advantages of wire-

actuated parallel manipulators, and extend and modify existing redundancy resolution techniques proposed by other researchers. The kinematic and dynamic modelling of an example planar wire-actuated parallel manipulator is developed in Section 2. The redundancy resolution schemes at the torque and velocity levels are given in Section 3 and Section 4, respectively. Simulation results at the torque and velocity levels are then developed in Section 5 and Section 6, respectively, in order to verify the effectiveness of the redundancy resolution techniques at the torque and velocity levels. The conclusion of the article is in Section 7.

2. MODELLING

The inverse dynamics of a planar wire-actuated parallel manipulator shown in Figure 1(a) is investigated. According to McColl and Notash [3], comparing the layouts of Figure 1(a) and Figure 1(b), the layout shown in Figure 1(a) offers a larger available static workspace and a larger range of orientations without interference problems between the wires and the mobile platform. So, the layout of Figure 1(a) is selected for the simulations. The dynamic problem is first formulated in the task space and then formulated in terms of the wire lengths and derivatives of wire lengths. Using the kinematic and dynamic analyses, the redundancy of the manipulator is resolved at the torque and velocity levels. Figure 1(c) shows the coordinates and parameters used for the analysis of the planar wire-actuated parallel manipulator shown in Figure 1(a). The fixed coordinate system $\Psi(X, Y)$, located at 0 , is attached to the base, while the moving coordinate system, $\Gamma(X', Y')$, is attached to the mobile platform at its centre of mass P with coordinates (x, y) in the base frame $\Psi(X, Y)$.

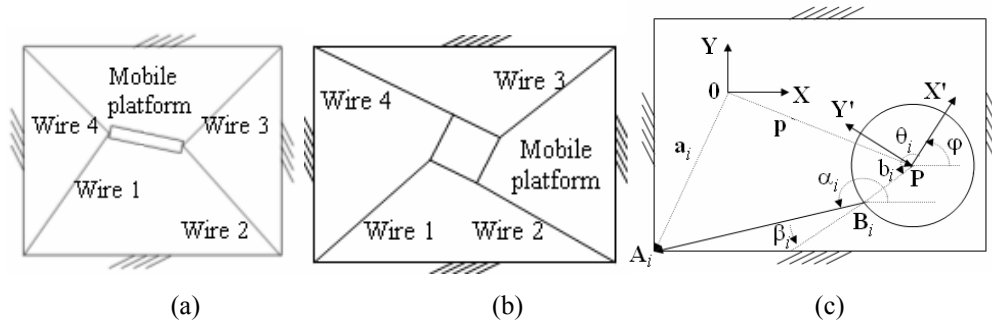


Figure 1. (a), (b) Example planar 3-DOF wire-actuated parallel manipulators (c) coordinates and variables.

The pose (position and orientation) of the mobile platform can be written as

$$\begin{bmatrix} x \\ y \\ \varphi \end{bmatrix} = \begin{bmatrix} a_{i_x} - l_{i_x} - b_i \cos(\theta_i + \varphi) \\ a_{i_y} - l_{i_y} - b_i \sin(\theta_i + \varphi) \\ \varphi \end{bmatrix}, \quad i = 1, \dots, n \quad (1)$$

where a_{i_x} and a_{i_y} are the coordinates of position vector \mathbf{a}_i of the anchor i in $\Psi(X, Y)$, l_i is the length of wire i , $l_{i_x} = l_i \cos \alpha_i$, $l_{i_y} = l_i \sin \alpha_i$, α_i is the direction for the axis of wire i , b_i is the distance between the mass centre P and the attachment point B_i of wire i on the mobile platform, θ_i is the orientation of line segments $\overline{PB_i}$ with respect to $\Gamma(X', Y')$, φ is the orientation of the mobile platform, and n (for a 3-DOF planar wire-actuated manipulator $n \geq 4$) is the number of wires.

Differentiating equation (1) results in

$$\begin{bmatrix} \dot{x} \\ \dot{y} \\ \dot{\phi} \end{bmatrix} = \begin{bmatrix} -c_i & l_i s_i & b_i s(\theta_i + \varphi) \\ -s_i & -l_i c_i & -b_i c(\theta_i + \varphi) \\ 0 & 0 & 1 \end{bmatrix} \begin{bmatrix} \dot{l}_i \\ \dot{\alpha}_i \\ \dot{\phi} \end{bmatrix}, \quad i=1, \dots, n \quad (2)$$

The solution of $[\dot{l}_i \quad \dot{\alpha}_i \quad \dot{\phi}]^T$ is given by

$$\begin{bmatrix} \dot{l}_i \\ \dot{\alpha}_i \\ \dot{\phi} \end{bmatrix} = \begin{bmatrix} -c_i & -s_i & b_i s(\theta_i + \varphi - \alpha_i) \\ s_i & -c_i & -b_i s(\theta_i + \varphi - \alpha_i) \\ l_i & l_i & l_i \end{bmatrix} \begin{bmatrix} \dot{x} \\ \dot{y} \\ \dot{\phi} \end{bmatrix}, \quad i=1, \dots, n \quad (3)$$

To relate wire length rates to the velocity of the mobile platform, the second and third rows of equation (3) are eliminated. So, the overall inverse velocity solution is written as

$$\begin{bmatrix} \dot{l}_1 \\ \vdots \\ \dot{l}_n \end{bmatrix} = - \begin{bmatrix} c_1 & s_1 & -b_1 s(\varphi + \theta_1 - \alpha_1) \\ \vdots & \vdots & \vdots \\ c_n & s_n & -b_n s(\varphi + \theta_n - \alpha_n) \end{bmatrix} \begin{bmatrix} \dot{x} \\ \dot{y} \\ \dot{\phi} \end{bmatrix} \quad (4)$$

where c_i , s_i and $s(\varphi + \theta_i - \alpha_i)$ stand for $\cos \alpha_i$, $\sin \alpha_i$ and $\sin(\varphi + \theta_i - \alpha_i)$, respectively, \dot{x} and \dot{y} are the components of linear velocities of the mobile platform and $\dot{\phi}$ is the angular velocity of the mobile platform, and \dot{l}_i is the length rate of wire i . The Jacobian matrix \mathbf{J} is defined as the negative of the coefficient of the mobile platform velocity in equation (4). So,

$$\mathbf{J} = \begin{bmatrix} c_1 & s_1 & -b_1 s(\varphi + \theta_1 - \alpha_1) \\ \vdots & \vdots & \vdots \\ c_n & s_n & -b_n s(\varphi + \theta_n - \alpha_n) \end{bmatrix} \quad (5)$$

It should be noted that within the context of serial manipulators the Jacobian matrix is referred to as the coefficient matrix of joint velocities. The alternate forward velocity solution of equation (4) is

$$[\dot{x} \quad \dot{y} \quad \dot{\phi}]^T = -\mathbf{J}^\# [\dot{l}_1 \quad \dots \quad \dot{l}_n]^T \quad (6)$$

where $\mathbf{J}^\#$ is the generalized (Moore-Penrose) inverse of \mathbf{J} , i.e., $\mathbf{J}^\# = (\mathbf{J}^T \mathbf{J})^{-1} \mathbf{J}^T$. It should be noted that using techniques based on the generalized inverse of matrices may, in general, lead to non-invariant and inconsistent results (i.e., results that are not invariant with respect to changes in the reference frame and/or changes in the dimensional units used to express the problem [11]). In such cases, the generalized inverse could be weighted using a suitable weighing metric to solve linear physical systems without producing inconsistencies and errors resulting from mixed physical units in the problem formulation. According to Doty et al. [11], when the left-hand side of equation (4) is unit consistent, $\mathbf{J}^\#$ is invariant to the choice of any weighing metric. So, using a weighing metric will not be required.

For the dynamic modelling, equation (6) is differentiated as

$$[\ddot{x} \quad \ddot{y} \quad \ddot{\phi}]^T = -\frac{d}{dt} \mathbf{J}^\# [\dot{l}_1 \quad \dots \quad \dot{l}_n]^T - \mathbf{J}^\# [\ddot{l}_1 \quad \dots \quad \ddot{l}_n]^T \quad (7)$$

From dynamic force and moment balances

$$\mathbf{J}^T \begin{bmatrix} \tau_1 \\ \vdots \\ \tau_n \end{bmatrix} = \begin{bmatrix} m\ddot{x} + F_{ext_x} \\ m\ddot{y} - mg + F_{ext_y} \\ I_z \ddot{\phi} + M_{ext_z} \end{bmatrix} \quad (8)$$

where m and I_z are the mass and the moment of inertia of the mobile platform respectively, $g = 9.81 \text{ m/s}^2$ is the gravitational constant, \ddot{x} and \ddot{y} are the components of linear accelerations and $\ddot{\phi}$ is the angular acceleration of the mobile platform, $[\tau_1 \dots \tau_n]^T$ is the vector of dynamic wire forces, F_{ext_x} and F_{ext_y} are the components of the external force acting on the mobile platform and M_{ext_z} is the external moment acting on the mobile platform about the z-axis. Assuming no external forces/moments are exerted on the mobile platform, equation (8) is simplified as

$$\mathbf{J}^T \begin{bmatrix} \tau_1 \\ \vdots \\ \tau_n \end{bmatrix} = \begin{bmatrix} m & 0 & 0 \\ 0 & m & 0 \\ 0 & 0 & I_z \end{bmatrix} \begin{bmatrix} \ddot{x} \\ \ddot{y} \\ \ddot{\phi} \end{bmatrix} + \begin{bmatrix} 0 \\ -mg \\ 0 \end{bmatrix} = \mathbf{M} \begin{bmatrix} \ddot{x} \\ \ddot{y} \\ \ddot{\phi} \end{bmatrix} + \mathbf{g} \quad (9)$$

where \mathbf{M} is the inertia matrix and \mathbf{g} is the vector of gravitational force. The solution to equation (9) is given by

$$[\tau_1 \dots \tau_n]^T = \mathbf{J}^{T\#} (\mathbf{M} [\ddot{x} \ \ddot{y} \ \ddot{\phi}]^T + \mathbf{g}) + (\mathbf{I} - \mathbf{J}^{T\#} \mathbf{J}^T) \mathbf{k} \quad (10)$$

The first term on the right-hand side of equation (10) is the minimum norm (particular) solution of equation (9) derived from the generalized inverse of matrix \mathbf{J}^T and $\mathbf{J}^{T\#}$ is the generalized inverse of \mathbf{J}^T , i.e., $\mathbf{J}^{T\#} = \mathbf{J}(\mathbf{J}^T \mathbf{J})^{-1}$, and the second term is the homogeneous solution that maps the free vector \mathbf{k} to the null space of \mathbf{J}^T [3, 4]. To simplify equation (10), the homogenous term could be written in terms of an arbitrary $n \times 1$ vector λ_τ multiplied by the kernel the transposed Jacobian [3, 4]

$$[\tau_1 \dots \tau_n]^T = \mathbf{J}^{T\#} (\mathbf{M} [\ddot{x} \ \ddot{y} \ \ddot{\phi}]^T + \mathbf{g}) + \ker(\mathbf{J}^T) \lambda_\tau \quad (11)$$

The determination of λ_τ depends on the optimization of a criterion function. The first term on the right-hand side of equation (11) is denoted as $\tau_p = \mathbf{J}^{T\#} (\mathbf{M} [\ddot{x} \ \ddot{y} \ \ddot{\phi}]^T + \mathbf{g})$.

To resolve the redundancy at the torque level, for given trajectories of the mobile platform, a λ_τ is identified (if it exists) at each instant such that minimum norm actuator forces/torques are achieved avoiding negative tension in the wires. It should be noted that throughout this paper, the term “norm” stands for the 2-norm, and all minimizations correspond to the 2-norm of the relevant vector.

The constraint tension function is

$$\boldsymbol{\tau} = \boldsymbol{\tau}_p + \ker(\mathbf{J}^T) \lambda_\tau \geq \mathbf{0} \quad (12)$$

Substituting equation (7) into equation (11) results in

$$[\tau_1 \dots \tau_n]^T = -\mathbf{J}^{T\#} \mathbf{M} \left(\frac{d}{dt} \mathbf{J}^\# \right) [\dot{l}_1 \dots \dot{l}_n]^T - \mathbf{J}^{T\#} \mathbf{M} \mathbf{J}^\# [\ddot{l}_1 \dots \ddot{l}_n]^T + \mathbf{J}^{T\#} \mathbf{g} + \ker(\mathbf{J}^T) \lambda_\tau \quad (13)$$

Equation (13) represents the inverse dynamic equation of the wire-actuated parallel manipulator in terms of wire lengths and their derivatives.

3. MINIMIZING WIRE TENSIONS FOR A GIVEN TRAJECTORY

To resolve redundancy at the torque level, given the trajectory of the mobile platform, it is required to know the Jacobian matrix at each time instant to construct the constraint function of equation (12) as a function of the decision variable λ_τ . So, the optimization problem is formulated as follows:

$$\begin{aligned} & \text{minimize } \boldsymbol{\tau}^T \boldsymbol{\tau} = \tau_1^2 + \dots + \tau_n^2 \\ & \text{subject to } \boldsymbol{\tau} = \boldsymbol{\tau}_p + \ker(\mathbf{J}^T) \lambda_\tau \geq \mathbf{0} \end{aligned} \quad (14)$$

and for each pose of the mobile platform, the value of λ_τ is calculated (if it exists) such that minimum positive wire tensions are maintained.

Given the trajectory of the mobile platform, $\mathbf{x}(t)=[x(t) \ y(t) \ \varphi(t)]^T$, and using the inverse velocity analysis, the Jacobian matrix at each time instant is calculated recursively. Using equation (4)

$$-\mathbf{J}|_{t_0} [\dot{x} \ \dot{y} \ \dot{\varphi}]_{t_1}^T = [\dot{l}_1 \ \dots \ \dot{l}_n]_{t_1}^T \quad (15)$$

and substituting the initial Jacobian matrix, $\mathbf{J}|_{t_0}$, and mobile platform trajectory at t_1 , $[\dot{x} \ \dot{y} \ \dot{\varphi}]_{t_1}^T$, the vector of wire length rates at t_1 , $[\dot{l}_1 \ \dots \ \dot{l}_n]_{t_1}^T$, is calculated. Following that, the vector of wire lengths \mathbf{l} at t_1 , $[l_1 \ \dots \ l_n]_{t_1}^T$ is obtained as

$$\mathbf{l}|_{t_1} = \dot{\mathbf{l}}|_{t_1} \Delta t + \mathbf{l}|_{t_0} \quad (16)$$

where $\dot{\mathbf{l}}$ is the vector of wire length rates, and Δt is the time increment. By substituting $\mathbf{l}|_{t_1}$ into equation (1), the orientation of wire i , α_i , at t_1 is derived. Therefore, the Jacobian matrix at t_1 is obtained.

By repeating the procedure, the Jacobian matrix at each time instant will be derived and substituted into equation (12) in order to identify λ_τ such that minimum positive wire tensions are maintained. As explained in equation (14), the objective function to be used in the optimization problem is to minimize the norm of tensions in the wires, i.e., minimum norm of λ_τ that guarantees positive tension in the wires.

4. RESOLVING REDUNDANCY WHEN MINIMIZING VELOCITY

In order to resolve redundancy at the torque level considering the minimization of the mobile platform velocity or minimizing the norm of wire length rates, equation (12) and the mobile platform velocity should be related. In fact, the trajectory of the mobile platform should be modified instantaneously such that minimum mobile platform velocity or minimum wire length rates is achieved subject to positive wire tensions. A similar approach was proposed by Oh and Agrawal [7] to minimize the sum of the norms for $\mathbf{x}(t)=[x(t) \ y(t) \ \varphi(t)]^T$ and its derivatives at specific time instants. They used a finite collocation grid in time to form a finite number of inequality constraints of equation (12). In the approach proposed in this section, the norm of the mobile platform velocity or wire length rates is minimized at each time instant.

In this approach, for a given mobile platform trajectory, $\mathbf{x}_o(t)=[x_o(t) \ y_o(t) \ \varphi_o(t)]^T$, the trajectory is modified at each time instant such that the objective function and the constraint function are satisfied. For this purpose, the mobile platform trajectory is chosen to have the following form

$$\mathbf{x}(t) = \begin{bmatrix} x \\ y \\ \varphi \end{bmatrix} = \begin{bmatrix} a_0 + a_1 t + a_2 t^2 + a_3 t^3 + a_4 t^3 (t_f - t) + a_5 t^3 (t_f - t)^2 \\ b_0 + b_1 t + b_2 t^2 + b_3 t^3 + b_4 t^3 (t_f - t) + b_5 t^3 (t_f - t)^2 \\ c_0 + c_1 t + c_2 t^2 + c_3 t^3 + c_4 t^3 (t_f - t) + c_5 t^3 (t_f - t)^2 \end{bmatrix} + \begin{bmatrix} p_1 \\ p_2 \\ p_3 \end{bmatrix} t^3 (t_f - t)^3 \quad (17)$$

where t_f is the final time instant, a_i , b_i and c_i are known constant coefficients, and p_1 , p_2 and p_3 are unknown variable coefficients (the values of p_1 , p_2 and p_3 will be calculated at each time instant). The first term on the right-hand side of equation (17) is denoted by vector $\mathbf{x}_o(t)=[x_o(t) \ y_o(t) \ \varphi_o(t)]^T$, and the second term by vector $\mathbf{x}_{\text{var}}(t, p_1, p_2, p_3)$. Differentiating equation (17) with respect to time results in

$$\dot{\mathbf{x}}(t) = \dot{\mathbf{x}}_o(t) + \dot{\mathbf{x}}_{\text{var}}(t, p_1, p_2, p_3) \quad (18)$$

where $\dot{\mathbf{x}}(t)$, $\dot{\mathbf{x}}_o(t)$ and $\dot{\mathbf{x}}_{\text{var}}$ are the time derivatives of $\mathbf{x}(t)$, $\mathbf{x}_o(t)$ and $\mathbf{x}_{\text{var}}(t)$, respectively. $\dot{\mathbf{x}}_{\text{var}}$ is referred to as the variable portion of the mobile platform velocity.

The fifth order $x_o(t)$, $y_o(t)$ and $\varphi_o(t)$ trajectories are chosen to satisfy eighteen initial and final boundary conditions of the mobile platform $\mathbf{x}(t)$ and its derivatives, i.e., $(x, \dot{x}, \ddot{x}, y, \dot{y}, \ddot{y}, \varphi, \dot{\varphi}, \ddot{\varphi})_0$ and $(x, \dot{x}, \ddot{x}, y, \dot{y}, \ddot{y}, \varphi, \dot{\varphi}, \ddot{\varphi})_f$, respectively. The eighteen coefficients a_i , b_i and c_i are defined from these eighteen boundary conditions. It should be noted that the addition of the second term on the right-hand side of equation (17), $\mathbf{x}_{\text{var}}(t, p_1, p_2, p_3)$, does not affect the boundary conditions of the mobile platform trajectories and their derivatives because of the chosen form of $t^3(t_f - t)^3$. Using this additional term on the right-hand side, the constraint function represented by equation (12) will become a function of p_1 , p_2 and p_3 , and in the optimization problem p_1 , p_2 and p_3 are changed such that the objective function is satisfied as well as achieving positive wire tensions. Three objective functions are defined and either of them could be used in order to resolve redundancy at velocity level. The objective functions are listed as

$$\text{minimizing } \dot{\mathbf{x}}^T \dot{\mathbf{x}} = \dot{x}^2 + \dot{y}^2 + \dot{\varphi}^2 \quad (19)$$

$$\text{minimizing } \dot{\mathbf{I}}^T \dot{\mathbf{I}} = \dot{l}_1^2 + \dots + \dot{l}_n^2 \quad (20)$$

$$\text{minimizing } \dot{\mathbf{x}}_{\text{var}}^T \dot{\mathbf{x}}_{\text{var}} \quad (21)$$

The objective function of equation (19) minimizes the norm of the mobile platform velocity. To compensate for the unit inconsistency of equation (19) (i.e., $(m/s)^2$ for \dot{x}^2 and \dot{y}^2 , and $(rad/s)^2$ for $\dot{\varphi}^2$), suitable weighing factors (e.g., the inertia matrix \mathbf{M}) can be used as the weighting matrix in order to minimize the weighted norm (e.g., minimizing $\dot{\mathbf{x}}^T \mathbf{M} \dot{\mathbf{x}}$, which has unit consistency) instead of $\dot{\mathbf{x}}^T \dot{\mathbf{x}}$. Since the first term on the right-hand side of equation (17) is constant, the first derivative of the second term (i.e., $\dot{\mathbf{x}}_{\text{var}}$) is used in the optimization problem of (21). The aim of using the first derivative of the variable term on the right-hand side of equation (17) (i.e., $\dot{\mathbf{x}}_{\text{var}}$) to define the third objective function, is to minimize $\dot{\mathbf{x}}_{\text{var}}$ such that $\dot{\mathbf{x}}(t)$ in equation (18) traces the given mobile platform velocity (i.e., $\dot{\mathbf{x}}_o(t)$) as close as possible. All three objective functions are subject to

$$\boldsymbol{\tau} = \boldsymbol{\tau}_p(t, p_1, p_2, p_3) + \ker(\mathbf{J}^T(t, p_1, p_2, p_3)) \boldsymbol{\lambda}_v \geq \mathbf{0} \quad (22)$$

So, after calculating p_1 , p_2 and p_3 , at each time instant, the minimum $\boldsymbol{\lambda}_v$ is calculated (if it exists) that maintains positive tension in all wires. Resolving redundancy at velocity level is only useful for applications in which the specified initial and final poses of the manipulator are of interest, such as pick and place, and spot welding. Since the trajectory is modified instantly the proposed redundancy resolution scheme could cause jerky motion in addition to discontinuity in wire tensions as the manipulator moves along the trajectory. Given the trajectory of the mobile platform as a function of p_1 , p_2 and p_3 , and using the inverse velocity analysis, the Jacobian matrix at each time instant is derived as a function of p_1 , p_2 and p_3 using a similar recursive procedure explained in Section 3. In other words, equation (15) can be rearranged as

$$-\mathbf{J}(t_j, p_1, p_2, p_3) \dot{\mathbf{x}}(t_{j+1}, p_1, p_2, p_3) = \dot{\mathbf{I}}(t_{j+1}, p_1, p_2, p_3) \quad (23)$$

and equation (16) as

$$\mathbf{I}(t_{j+1}, p_1, p_2, p_3) = \dot{\mathbf{I}}(t_{j+1}, p_1, p_2, p_3) \Delta t + \mathbf{I}(t_j, p_1, p_2, p_3) \quad (24)$$

By substituting $\mathbf{I}(t_{j+1}, p_1, p_2, p_3)$ into equation (1), $\cos \alpha_i$ and $\sin \alpha_i$ at t_{j+1} are obtained as functions of p_1 , p_2 and p_3 and as a result the Jacobian matrix at t_{j+1} is derived as a function of p_1 , p_2 and p_3 . $\mathbf{J}(t_{j+1}, p_1, p_2, p_3)$ is then substituted into equation (22),

$$\boldsymbol{\tau}(t_{j+1}, p_1, p_2, p_3) = \boldsymbol{\tau}_p(t_{j+1}, p_1, p_2, p_3) + \ker(\mathbf{J}^T(t_{j+1}, p_1, p_2, p_3))\boldsymbol{\lambda}_v \geq \mathbf{0} \quad (25)$$

in order to identify p_1 , p_2 , p_3 and $\boldsymbol{\lambda}_v$ such that the objective function is satisfied maintaining positive tension. In fact, p_1 , p_2 and p_3 appearing in the objective function are changed such that either the norms of $\dot{\mathbf{I}}\dot{\mathbf{I}}$ or $\dot{\mathbf{x}}^T\dot{\mathbf{x}}$ or $\dot{\mathbf{x}}_{\text{var}}^T\dot{\mathbf{x}}_{\text{var}}$ are increased until positive tension in the wires is achieved.

5. SIMULATION RESULTS WHEN MINIMIZING WIRE TENSIONS

In this section, the simulation results of redundancy resolution of the planar wire-actuated manipulator, shown in Figure 1(a), are presented. The optimization problem is formulated as follows:

$$\begin{aligned} & \text{minimize } \boldsymbol{\tau}^T \boldsymbol{\tau} = \tau_1^2 + \tau_2^2 + \tau_3^2 + \tau_4^2 \\ & \text{subject to } \boldsymbol{\tau} = \boldsymbol{\tau}_p + \ker(\mathbf{J}^T)\boldsymbol{\lambda}_\tau \geq \mathbf{0} \end{aligned} \quad (26)$$

and for each pose of the mobile platform, a value $\boldsymbol{\lambda}_\tau$ is calculated (if it exists) such that minimum positive wire tensions are maintained. With four wires, the constraint function of equation (12) is reduced to four linear inequalities in terms of $\boldsymbol{\lambda}_\tau$, where $\boldsymbol{\lambda}_\tau$ is reduced to a scalar. The optimization problem of the four-wire-actuated manipulator shown in Figure 1(a) is carried out in Matlab using the *fmincon* function to verify the optimization procedure discussed in Section 3.

The following coordinates $\{(-4, -3), (4, -3), (4, 3), (-4, 3)\}$ (units in meters) are used for anchor position vectors $\{\mathbf{a}_1, \mathbf{a}_2, \mathbf{a}_3, \mathbf{a}_4\}$ in the fixed frame, and the orientations of line segments \overline{PB}_i with respect to the mobile platform frame, $\{\theta_1, \theta_2, \theta_3, \theta_4\}$, are $\{180^\circ, 0^\circ, 0^\circ, 180^\circ\}$. The mass m and radius b_i of the mobile platform are 2 kg and 0.5 m, respectively. The mass moment of inertia of the mobile platform, I_z , is 0.0144 kg.m². The initial and final boundary conditions $(x, \dot{x}, y, \dot{y}, \phi, \dot{\phi})_{0,f}$ are assumed to be $(0, 0, 0, 0, 0, 0)_0$ and $(1\text{ m}, 0, 1\text{ m}, 0, 5^\circ, 0)_f$, respectively, with $t \in [0, 1]\text{ s}$ and time step of $\Delta t = 0.001\text{ s}$. For the sake of simulation and simplifications, the initial and final acceleration components of the mobile platform are not included in the boundary conditions, and a third order polynomial is used for the mobile platform trajectory satisfying twelve boundary conditions of $\mathbf{x}(t)$, and its derivative.

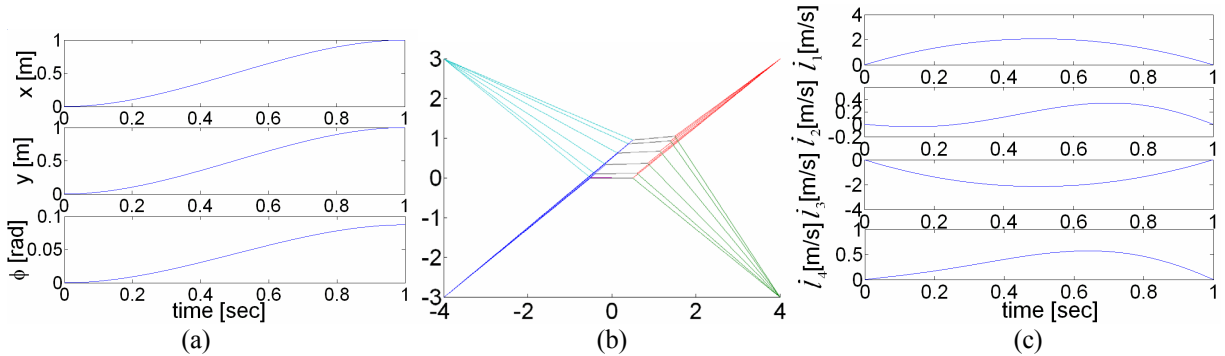


Figure 2. (a) Pose of the mobile platform, (b) configuration change of the mobile platform, (c) wire length rates.

Figure 2(a) and Figure 2(b) show the defined motion of the mobile platform, regardless of whether positive tension in the wires is achieved or not. Figure 2(c) represents the wire length rates calculated using equation (15). It should be noted that the determination of wire length rates is independent of the optimization of the tension in the wires. Figure 3(a) shows the minimum $\boldsymbol{\lambda}_\tau$ that guarantees positive tension in the wires. Since the change in the orientation of the mobile platform is small enough (i.e., 5 deg) the optimization was terminated successfully. If the change in the orientation of the mobile platform is not small enough, the pose

of the mobile platform may not lie within the available workspace of the manipulator and the tension constraints may not be met. The plots of the particular solutions τ_p (i.e., without null space contribution) are given in Figure 3(b). As it can be seen, tensions in the third and fourth wires are negative. To maintain positive tensions in the third and fourth wires, null space contribution is used. Figure 3(c) illustrates the tension histories resulting from the substitution of minimum λ_r (shown in Figure 3(a)) into equation (12).

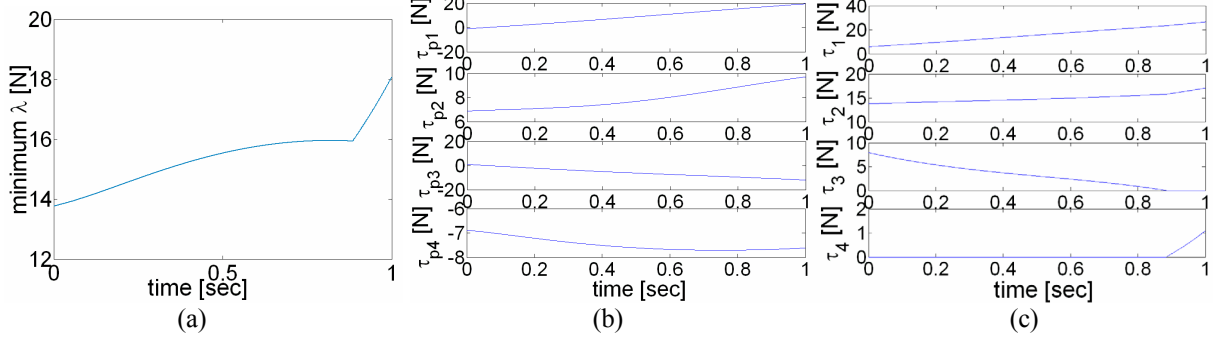


Figure 3. (a) Minimum λ_r to maintain positive tension in the wires, (b) tension in the wires without null space contribution, (c) wire tensions with null space contribution.

6. SIMULATION RESULTS WHEN MINIMIZING VELOCITY

In this section, the simulation results of redundancy resolution of the planar wire-actuated manipulator, shown in Figure 1(a), are presented. For a given mobile platform trajectory, $\mathbf{x}_o(t) = [x_o(t) \ y_o(t) \ \varphi_o(t)]^T$ of equation (17), the trajectory is modified at each time instant such that:

$$\begin{aligned} & \text{minimize } \dot{\mathbf{x}}_{\text{var}}^T \dot{\mathbf{x}}_{\text{var}} & (27) \\ & \text{subject to } \boldsymbol{\tau} = \boldsymbol{\tau}_p + \ker(\mathbf{J}^T) \boldsymbol{\lambda}_v \geq \mathbf{0} \end{aligned}$$

and a value is calculated for p_1 , p_2 , p_3 and λ_v (if it exists), instantaneously, that maintains positive tension in the wires. With four wires, the constraint function of equation (22) is reduced to four linear inequalities in terms of λ_v where λ_v is reduced to a scalar. The optimization problem of the four-wire-actuated manipulator shown in Figure 1(a) is carried out in Matlab using the *fmincon* function to verify the optimization procedure discussed in Section 3.

The following coordinates $\{(-1, -0.75), (1, -0.75), (1, 0.75), (-1, 0.75)\}$ (units in meters) are used for the anchor position vectors $\{\mathbf{a}_1, \mathbf{a}_2, \mathbf{a}_3, \mathbf{a}_4\}$ in the fixed frame, and the orientations of line segments \overline{PB}_i with respect to the mobile platform frame, $\{\theta_1, \theta_2, \theta_3, \theta_4\}$, are $\{180^\circ, 0^\circ, 0^\circ, 180^\circ\}$. The mass m and radius b_i of the mobile platform are 2 kg and 0.25 m, respectively. The mass moment of inertia of the mobile platform, I_z , is 0.0144 kg.m². The initial and final boundary conditions $(x, \dot{x}, \ddot{x}, y, \dot{y}, \ddot{y}, \varphi, \dot{\varphi}, \ddot{\varphi})_{0,f}$ are assumed to be $(0, 0, 0, 0, 0, 0, 10^\circ, 0, 0)_0$ and $(0, 0, 0, 0.5 \text{ m}, 0, 0, 10^\circ, 0, 0)_f$, respectively, with $t \in [0, 1] \text{ s}$ and time step of $\Delta t = 0.001 \text{ s}$. Figure 4(a) and Figure 4(b) show the motion of the mobile platform regardless of whether positive tension in the wires is achieved or not. From Figure 4, it can be seen that the mobile platform moves upward until it reaches its predefined final position and orientation. There are fluctuations in the plots of x and φ in Figure 4(a). According to the boundary conditions, it may be expected that during the motion of the mobile platform, the only change in the pose of the mobile platform will be the change in the y -direction. However, due to the optimization problem satisfying equation (27), not only does the y coordinate of the

mobile platform change during the motion of the mobile platform, but so do x and ϕ , until the predefined final boundary conditions are achieved. As it can be seen from Figure 4(a), the maximum change in x and ϕ are approximately 1 mm and 0.08 deg, respectively.

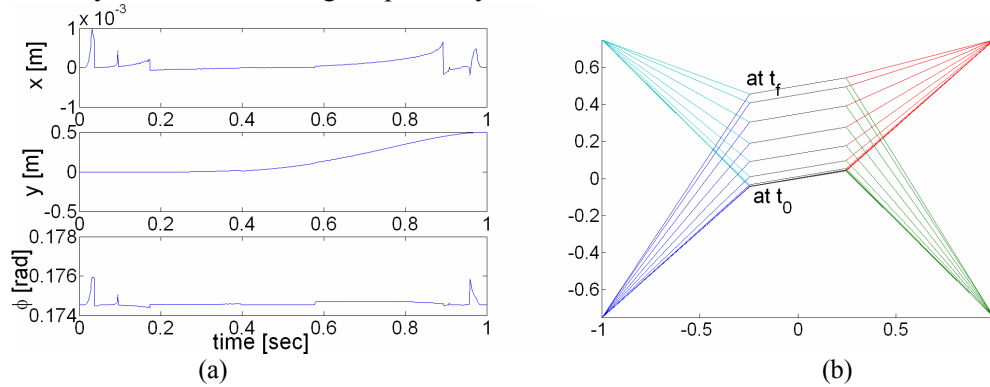


Figure 4. (a) Pose of the mobile platform, (b) change in the configuration of the mobile platform.

Figure 5 shows the actual velocity of the mobile platform $\dot{\mathbf{x}}(t)$ and the predefined component of mobile platform velocity $\dot{\mathbf{x}}_o(t)$ and the variable portion of the mobile platform velocity $\dot{\mathbf{x}}_{\text{var}} = \dot{\mathbf{x}}(t) - \dot{\mathbf{x}}_o(t)$. The coefficients a_i , b_i and c_i are determined from the eighteen predefined boundary conditions $(x, \dot{x}, \ddot{x}, y, \dot{y}, \ddot{y}, \phi, \dot{\phi}, \ddot{\phi})_{0,f}$ with $t \in [t_0, t_f]$. From the optimization problem represented by equation (27), it is desired that the actual velocity of the mobile platform, $\dot{\mathbf{x}}(t)$, be as close to $\dot{\mathbf{x}}_o(t)$ as possible. The variable portion of the mobile platform velocity illustrated in Figure 5(c) shows whether $\dot{\mathbf{x}}(t)$ is close to $\dot{\mathbf{x}}_o(t)$ or not.

The peaks in the plots of \dot{x} and $\dot{\phi}$ (Figure 5(a)) are due to fluctuations in x and ϕ in Figure 4(a). As it can be seen from Figure 5(a), the solution of equation (27) has resulted in velocity components which are point-wise feasible but with jumps at some time instants. From an experimental point of view, it may become important for the solution to be continuous to avoid instability and jerky motion of the mobile platform. The two main velocity peaks in the x and y directions occur approximately at 0.03 s and 0.96 s. Since at each time instant a new set of p_1 , p_2 , p_3 and λ_v that satisfies the objective and constraint functions is calculated, there is no guarantee that the solutions of p_1 , p_2 , p_3 and λ_v are continuous. For instance, at 0.03 s and 0.96 s, the solutions of p_1 , p_2 , p_3 and λ_v that ensure minimum $\dot{\mathbf{x}}_{\text{var}}^T \dot{\mathbf{x}}_{\text{var}}$ and positive tension in the wires, have caused peaks in the values of p_1 , p_2 and p_3 . An approach to avoid discontinuity is the globally continuous solution proposed by Oh and Agrawal [7] that determines a specific set of p_1 , p_2 , p_3 and λ_v , for the entire motion of the mobile platform using discrete poses of the mobile platform along the path. They used trajectory parameterization in conjunction with a finite collocation grid in time to ensure smooth tensions during the path. However, it should be noted that their proposed solution minimizes the mobile platform velocity but not at each time instant, i.e., $\dot{\mathbf{x}}(t)$ in equation (18) traces $\dot{\mathbf{x}}_o(t)$ as close as possible but not at each time instant. Figure 6(a) shows the solutions of p_1 , p_2 , p_3 and λ_v that guarantee positive tension in the wires. The two main peaks in the plots of p_1 , p_2 and p_3 (shown in Figure 6(a)) have affected velocity components \dot{x} and $\dot{\phi}$ (shown in Figure 5(a)) at 0.03 s and 0.96 s. Figure 6(b) illustrates the tension histories resulting from the substitution of p_1 , p_2 , p_3 and λ_v (shown in Figure 6(a)) into equation (25). As it can be seen from Figure 6(b), the tension in the fourth wire is approximately zero (order of 10^{-15}). Using a threshold for wire tensions, the minimum allowable tension in the wires could be defined. In the optimization problem

used in this work (equation (27)), the minimum tension in the wires was considered to be zero (resulting in fluctuations around zero for the fourth wire tension). Figure 6(c) represents the wire length rates resulted from the substitution of p_1 , p_2 , p_3 and λ_v (shown in Figure 6(a)) into equation (23). Considering Figure 4(b) and Figure 6(c), as the mobile platform moves upward the first two wires are extended whereas wires 3 and 4 are shortened.

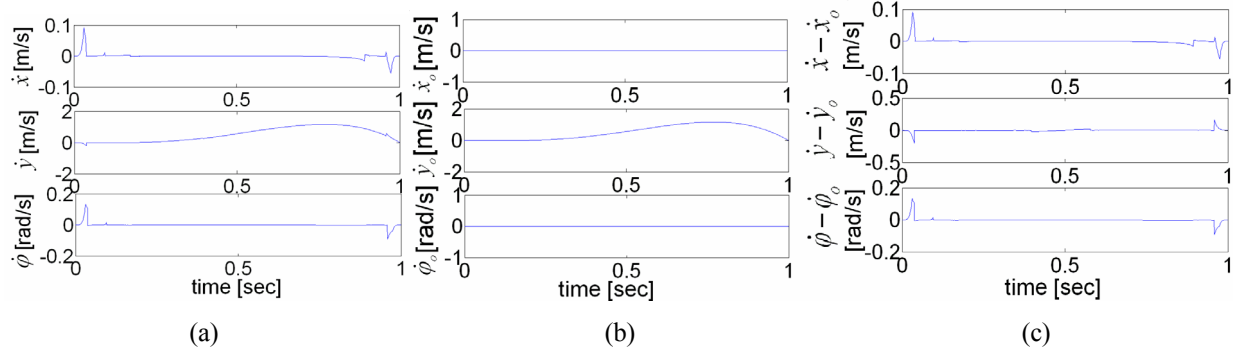


Figure 5. Components of mobile platform velocity: (a) actual velocity of the mobile platform, i.e., $\dot{\mathbf{x}}(t)$ (b) predefined component of mobile platform velocity, i.e., $\dot{\mathbf{x}}_o(t)$, (c) variable portion of the mobile platform velocity, i.e., $\dot{\mathbf{x}}_{\text{var}} = \dot{\mathbf{x}}(t) - \dot{\mathbf{x}}_o(t)$.

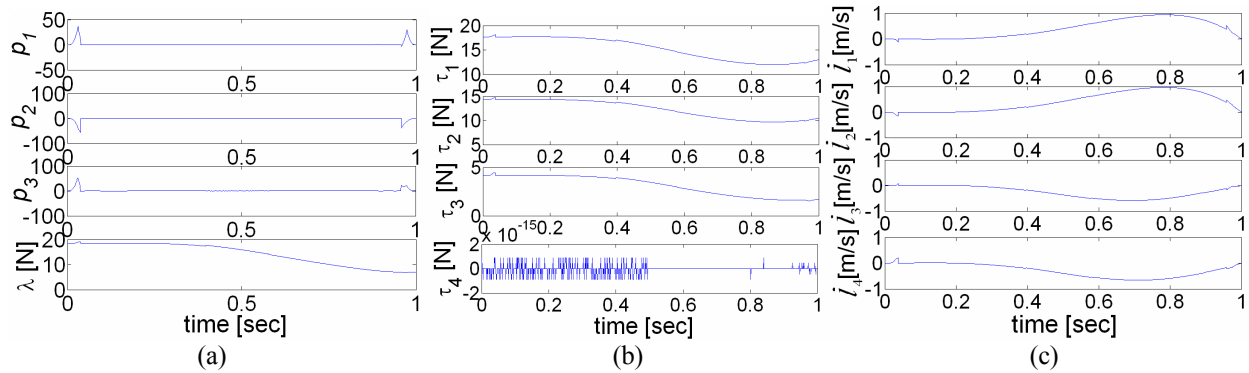


Figure 6. (a) Solutions of p_1 , p_2 , p_3 and λ_v to maintain positive tensions in the wires, (b) tension in the wires with null space contribution, (c) wire length rates.

7. DISCUSSION AND CONCLUSIONS

In this paper, two approaches to resolve actuation redundancy of planar wire-actuated parallel manipulators were investigated. In the first approach, a prescribed trajectory of the mobile platform was followed and the norm of wire tensions was minimized while maintaining positive tension in the wires. In the second approach, the desired mobile platform trajectory was modified instantaneously such that the minimum norm velocity of the mobile platform or minimum norm wire length rates was achieved, subject to positive wire tensions. Simulations of a 3-DOF planar wire-actuated parallel manipulator was developed minimizing either the norm of wire tensions or the norm of the variable portion of the mobile platform velocity. Based on the optimization results, it was observed that using the null space contribution the wire tensions can be kept positive successfully. However, it should be noted that this is not always the case, e.g., when the manipulator does not allow large orientations and the change in the orientation of the mobile platform is not small enough. It was also shown that some redundancy resolution schemes may result in fluctuations in the actuator torques/forces or in the wire length rates and velocity of the mobile platform. Based on the optimization criterion and the optimization scheme, the torque level approach used a continuous mobile platform trajectory and produced

continuous wire tensions, while the velocity level approach produced fluctuations in the mobile platform trajectory. The wire tensions produced at the velocity level were continuous. So, the choice of a proper optimization scheme depends on the application of the manipulator. For example, resolving redundancy at velocity level is, in general, recommended for trajectory planning [7] and/or for applications when the specified initial and final poses of the manipulator and/or initial and final velocities and accelerations of the mobile platform are of interest. Comparing the two described redundancy resolution techniques, the computational procedure at the torque level is faster and less complicated than that at velocity level.

REFERENCES

- [1] S. Kawamura, K. Hitoshi, and W. Choe, "High-speed manipulation by using parallel wire-driven robots," *Robotica*, vol. 18, pp. 13-21, 2000.
- [2] W. Choe, K. Hitoshi, K. Katsuta, and S. Kawamura, "A Design of Parallel Wire Driven Robots for Ultrahigh Speed Motion Based on Stiffness Analysis," in *Proceedings of the Japan USA Symposium on Flexible Automation*, K. Stelson and F. Oba, Eds.: The American Society of Mechanical Engineers, 1996, pp. 159-166.
- [3] D. McColl and L. Notash, "Configuration and Workspace Analysis of Planar Wire-Actuated Parallel Manipulators," *Proceedings of the 17th CISM-IFTOMM Symp. Robot Design, Dynamics, and Control (RoManSy)*, 2008.
- [4] D. McColl and L. Notash, "Workspace Analysis of Planar Wire-Actuated Parallel Manipulators Using Antipodal Grasp Theorem," *Proceedings of the CSME Forum*, pp. 6 pages, 2008.
- [5] R. L. Williams II and P. Gallina, "Translational Planar Cable-Direct-Driven Robots," *Journal of Intelligent and Robotic Systems*, vol. 37, pp. 69-96, 2003.
- [6] R. L. Williams II, P. Gallina, and J. Vadia, "Planar Translational Cable-Direct-Driven Robots," *Journal of Robotic Systems*, vol. 20, pp. 107-120, 2003.
- [7] S.-R. Oh and S. K. Agrawal, "Cable Suspended Planar Robots with Redundant Cables: Controllers with Positive Tensions," *IEEE Transactions on Robotics*, vol. 21, pp. 457-465, 2005.
- [8] L. Notash and A. Kamalzadeh, "Inverse dynamics of wire-actuated parallel manipulators with a constraining linkage," *Mechanism and Machine Theory*, vol. 42, pp. 1103-1118, 2007.
- [9] M. Gouttefarde and C. M. Gosselin, "Analysis of the Wrench-Closure Workspace of Planar Parallel Cable-Driven Mechanisms," *IEEE Transactions on Robotics*, vol. 22, pp. 434-445, 2006.
- [10] S. Bouchard, C. e. M. Gosselin, and B. Moore, "On the Ability of a Cable-Driven Robot to Generate a Prescribed Set of Wrenches," *Proceedings of IDETC/CIE 2008, ASME 2008 International Design Engineering Technical Conferences & Computers and Information in Engineering Conference*, pp. 1-12, 2008.
- [11] K. I. Doty, C. Melchiorri, and C. Bonivento, "A Theory of Generalized Inverses Applied to Robotics," *Int. J. Robotics Research*, vol. 12, pp. 1-19, 1995.